Gene Therapy (2016) **23**, 606–614

www.nature.com/gt

OPEN

ORIGINAL ARTICLE

Development of an AAV9 coding for a 3XFLAG-TALE$_{frat\#8}$-VP64 able to increase *in vivo* the human frataxin in YG8R mice

P Chapdelaine[1,2], C Gérard[1,2], N Sanchez[1,2], K Cherif[1,2], J Rousseau[1,2], DL Ouellet[1,2], D Jauvin[1,2] and JP Tremblay[1,2]

Artificially designed transcription activator-like effector (TALE) proteins fused to a transcription activation domain (TAD), such as VP64, are able to activate specific eukaryotic promoters. They thus provide a good tool for targeted gene regulation as a therapy. However, the efficacy of such an agent *in vivo* remains to be demonstrated as the majority of studies have been carried out in cell culture. We produced an adeno-associated virus 9 (AAV9) coding for a TALE$_{frat\#8}$ containing 13 repeat variable diresidues able to bind to the proximal promoter of human frataxin (*FXN*) gene. This TALE$_{frat\#8}$ was fused with a 3XFLAG at its N terminal and a VP64 TAD at its C terminal, and driven by a CAG promoter. This AAV9_3XFLAG-TALE$_{frat\#8}$-VP64 was injected intraperitoneally to 9-day-old and 4-month-old YG8R mice. After 1 month, the heart, muscle and liver were removed and their FXN mRNA and FXN protein were analyzed. The results show that the AAV9_3XFLAG-TALE$_{frat\#8}$-VP64 increased the FXN mRNA and FXN protein in the three organs studied. These results corroborate our previous *in vitro* studies in the FRDA human fibroblasts. Our study indicates that an AAV coding for a TALE protein coupled with a TAD may be used to increase gene expression *in vivo* as a possible treatment not only for FRDA but also for other haploinsufficiency diseases.

Gene Therapy (2016) **23,** 606–614; doi:10.1038/gt.2016.36

INTRODUCTION

In the eukaryotic cells,[1] the regulation of the expression of the key gene involved in an haploinsufficiency disease could be modulated by artificial transcription factors (ATFs).[2] Zinc-finger proteins (ZFPs), transcription activator-like effectors (TALEs) and dCas9 fused with a transcription activation domain (TAD) are three types of ATFs available to mediate not only site-specific DNA recognition but also gene expression regulation.[2] TALEs are natural effector proteins secreted by pathogenic bacteria genus *Xanthomonas* that can bind and regulate host gene expression in the plants.[3,4] The middle region of TALE protein contains repetitive segments of 33 or 34 amino acids containing different amino acids in positions 12 and 13 (called repeat variable diresidues, RVDs), which determine the DNA binding site even in mammalian cells.[5–7] TADs, such as VP16, VP64, VP160 or p65, may be attached to the TALE target-binding domain, making a custom genome engineering protein able in principle to specifically control the expression of any human gene when the TALE is targeting its promoter.[7]

The main hurdle for a clinical application of this ATF technology is the development of an optimal delivery method for this new gene therapy approach. Transfection of plasmids encoding ZFPs and more recently TALEs and the CRISPR/Cas9 system has been successfully carried out *in vitro* by electroporation or cationic lipid-based methods in different cell types, but these procedures have limited efficacy and may be toxic.[8] Viral vectors for ATF delivery may be an alternative to a non-viral delivery system, especially *in vivo*.[8] Among the viral vectors known to accommodate the delivery of zinc-finger nucleases are the lentiviruses (LVs)[9] and the AAVs.[10] However, there are only few reports on the *in vivo* delivery of TALE nucleases (TALENs).[11] Artificially designed TALEs may be fused not only to a nuclease such as FokI for genome editing but also to a TAD such as VP64 to upregulate specific genes.[12] Recently, LVs failed to deliver TALENs in target cells,[13] but LVs lacking reverse transcriptase expression improved the delivery of TALENs *in vitro*, thus avoiding the RVD recombination.[14] However, *in vivo* delivery of TALENs remains to be carried out. AAVs have been suggested for TALEN delivery but because of the limited AAV packaging capacity, ~4.7 kb, two vectors are required to deliver a TALEN pair required for genome editing.[11] However, the use of TALE-VP64 as ATF requires only one AAV vector and should provide a stable expression to induce an *in vivo* potent and long-term increase of a specific gene expression. AAVs are non-pathogenic and are able to transduce dividing and non-dividing cells. They have already been tested in several gene therapy trials and have become the platform of choice for *in vivo* gene transfer.[2] A wide variety of AAV serotypes have been recently isolated,[15] and among them, AAV9 has been shown to produce robust expression, particularly in cardiomyocytes.[16] Moreover, AAV9 is also able to deliver genes in the brain following systemic delivery.[17–19]

Friedreich's ataxia (FRDA) is a hereditary disease due to an increased number of GAA trinucleotide repeats in the intron 1 of the frataxin (*FXN*) gene. This mutation leads to a reduced expression of the mitochondrial FXN protein, resulting in oxidative stress in all cells inducing death, particularly of cardiomyocytes and neurons.[20–22] Our laboratory has recently focused on the

[1]Unité de Génétique Humaine, Axe Neurosciences, Centre de Recherche du Centre Hospitalier de Universitaire de Québec-Université Laval, Québec City, QC, Canada and [2]Department of Molecular Medicine, Faculty of Medicine, Laval University, Quebec City, QC, Canada. Correspondence: Professor JP Tremblay, Unité de Génétique humaine, Axe Neurosciences, Centre de Recherche du Centre Hospitalier Universitaire de Universitaire de Québec-Université Laval, CRCHUL 2705 Boulevard Laurier, Room P09300, Québec City, QC, Canada G1V4G2.
E-mail: Jacques-P.Tremblay@crchul.ulaval.ca
Received 22 November 2015; revised 9 March 2016; accepted 7 April 2016; accepted article preview online 15 April 2016; advance online publication, 5 May 2016

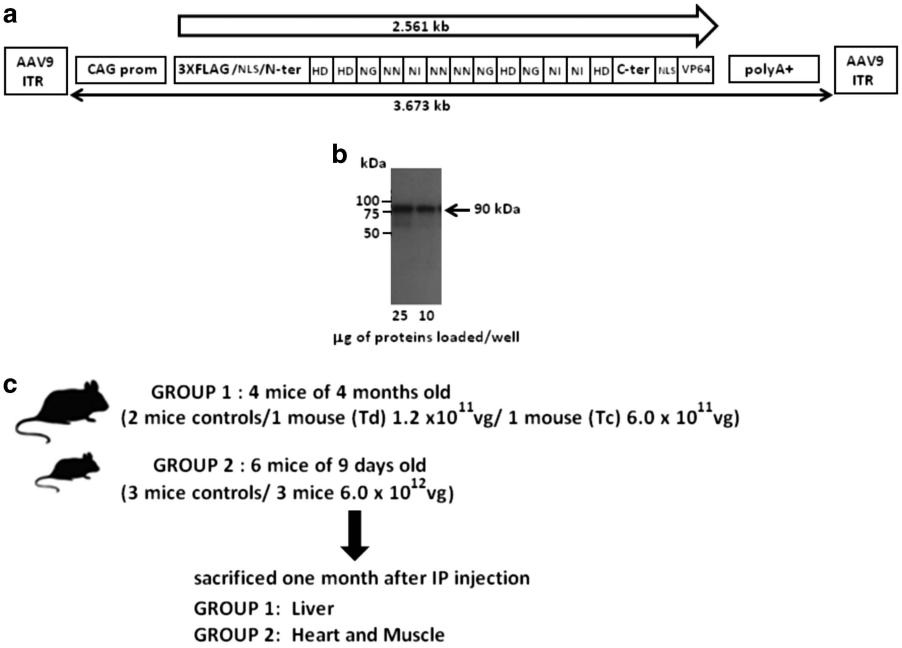

Figure 1. Schema of the AAV9_3XFLAG-TALE$_{frat\#8}$-VP64, detection of the transgenic protein and vector delivery protocol. (**a**) The plasmid contains the AAV-ITRs and the CAG promoter driving the 3XFLAG-TALE$_{frat\#8}$-VP64 transgene (3.6 kb). The TALE contains 13 RVDs and 2 nuclear localization signals (NLS). This plasmid was used to produce the AAV serotype 9 vector. (**b**) The transgenic protein expression in 293 T cells transfected with pAAV9 TALE$_{frat\#8}$-VP64 was detected by western blot with an anti-FLAG antibody. Total proteins of 10 and 25 µg were loaded in two wells, electrophoresed on a 10% SDS-polyacrylamide gel and electrotransferred on nitrocellulose membrane for the western blot. (**c**) Two groups of mice were used to realize the present study. Group 1 was composed of four 4-month-old YG8R mice, including two control mice injected intraperitoneally with saline and two mice injected intraperitoneally with 1.2×10^{11} or 6×10^{11} vg of AAV9_3XFLAG-TALE$_{frat\#8}$-VP64. Group 2 composed of six 9-day-old YG8R mice, including three control mice injected intraperitoneally with saline and three mice injected intraperitoneally with 6×10^{12} vg of AAV9_3XFLAG-TALE$_{frat\#8}$-VP64. All mice were killed 1 month later.

development of a new gene therapy for this disease using an AAV vector coding for 3XFLAG-TALE$_{frat\#8}$-VP64. This TALE targets the human FXN promoter and increased by 1.7- to 2-fold the FXN mRNA and FXN protein levels in FRDA fibroblasts having alleles containing 541 and 420 GAA repeats.[1] The aim of the present work was to evaluate the feasibility of using this TALE to increase transcription *in vivo*. The 3XFLAG-TALE$_{frat\#8}$-VP64 gene was thus introduced in an AAV9 able to transfer efficiently a gene in the mouse heart and skeletal muscles.[16] We used for these experiments the YG8R mouse containing a transgene derived from an FRDA patient with a long GAA repeat. The FXN mRNA and protein levels are thus reduced in this model, causing some typical phenotypes of this haploinsufficiency disease. In the present study, we demonstrated an increase in the FXN mRNA and protein mainly in the heart and the skeletal muscles 1 month after intraperitoneal injection of the AAV9_3XFLAG-TALE$_{frat\#8}$-VP64 to 9-day-old YG8R mice. Following similar injections in 4-month-old YG8R mice, such increases were observed mainly in the liver. These observations illustrate the interest in delivering with AAV TALE ATFs as a therapy for haploinsufficiency diseases.

RESULTS

Structure of AAV9 3XFLAG-TALE$_{frat\#8}$-VP64 and protein expression

Figure 1a represents the scheme of the AAV9 containing the 3XFLAG-TALE$_{frat\#8}$-VP64 under the control of the CAG promoter (*C*MV early enhancer element, first exon and first intron of β-*A*ctin and the splice acceptor of the rabbit β-*G*lobin gene). The AAV9_3XFLAG-TALE$_{frat\#8}$-VP64 plasmid was initially successfully tested in 293 T cells to verify by western blot with an anti-FLAG antibody the expression of a protein of expected molecular weight (i.e., ~ 90 kDa) (Figure 1b). The AAV9 vector was injected intraperitoneally with 1.2×10^{11} vg (viral genome) or with

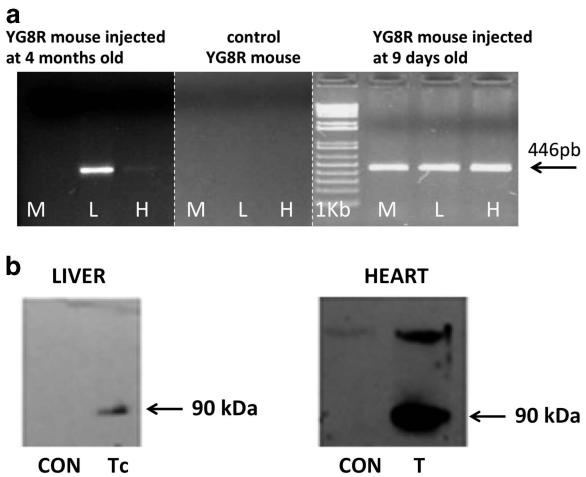

Figure 2. (**a**) Detection of AAV9_3XFLAG-TALE$_{frat\#8}$-VP64 transgene and protein in the muscle, heart and liver of YG8R mice. Muscle (M), liver (L) and heart H) were removed from 4-month-old mice treated with 6×10^{11} vg (left panel), from 9-day-old mice treated with 6×10^{12} vg (right panel) or from control mice injected with saline (middle panel). The expected 446 pb PCR product was strongly detectable in the liver but barely detectable in the muscles and heart of 4-month-old mice. The amplicon was also strongly detected in the three tissues of the 9-day-old mice. (**b**) Proteins extracted from the liver of 4-month-old (left panel) and from the heart of 9-day-old (right panel) YG8R mice were loaded on a 10% SDS-polyacrylamide gel. In both panels, the left lane contains proteins from a control mouse treated with saline and the right lane contains proteins from mice injected intraperitoneally with AAV9_3XFLAG-TALE$_{frat\#8}$-VP64. The transgenic protein (90 kDa) was detected by western blot with a monoclonal antibody against the 3XFLAG in tissues of treated mice but not in control tissues.

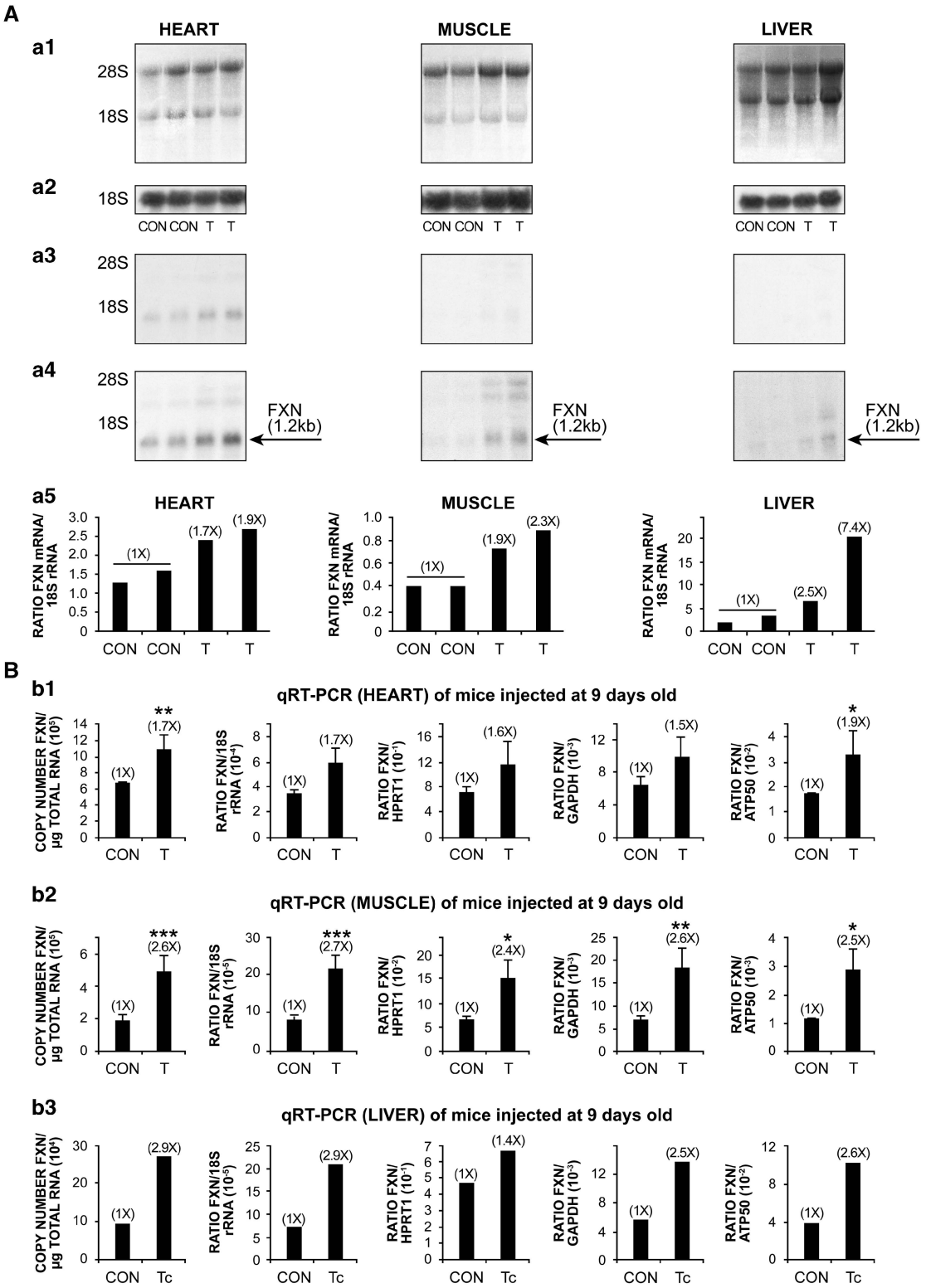

Figure 3. (**A**) Effect of the treatment of AAV9_3XFLAG-TALE$_{frat\#8}$-VP64 on the FXN mRNA analyzed by Northern blots and qRT-PCR in YG8R mice. The treatments were carried out at different doses of AAV9: T indicates 6×10^{12} vg per mouse, Tc 6×10^{11} vg per mouse and 1.2×10^{11} vg per mouse. The top figures (a1) are total RNA electrophoresed on 1.2% agarose-formaldehyde gel. These RNAs were extracted from three tissues: heart, muscle of group 2 and liver of group 1 YG8R mice. (a2–a4) Northern blot analyses. (a2) Signal hybridization of 18 S rRNA (used as internal standard). (a3 and a4) The hybridization signal of the FXN mRNA exposed for different times, 2 days (a3) and 10 days (a4). (a5) Histograms corresponding to (a4). The Northern blots suggest increased FXN mRNA in mice treated with the recombinant virus. (**B**) Three horizontal panels summarize the FXN qRT-PCR results. The top panels (b1 and b2) represent histograms showing increased of FXN mRNA in the heart and muscle (group 2, $N=3$, ave. $\pm$ s.d. *for $P<0.05$, **for $P<0.01$ and *** for $P<0.005$). The results are expressed either as copy number or as ratios relative to 18 S rRNA, GAPDH, ATP50 and HPRT1. The middle panel (b2) represents FXN mRNA expressed in the muscle (group 2). The lower panel (b3) illustrates FXN mRNA expressed in the liver (group 1), but the histogram bar represents only one mouse for control and one mouse treated with recombinant virus (Tc).

6×10^{11} vg to two 4-month-old mice (group 1; Figure 1c) and with 6×10^{12} vg to three 9-day-old mice (group 2; Figure 1c). Two controls in group 1 and three controls in group 2 were injected with saline. The liver from the four mice in group 1 and the heart and the skeletal muscles from the six mice in group 2 were collected 1 month after the injection. The effect of AAV9_3XFLAG-TALE$_{frat\#8}$-VP64 on the FXN expression in these tissues was then investigated.

Detection of 3XFLAG-TALE$_{frat\#8}$-VP64 transgene and protein in some tissues of YG8R mice

A total of 1.2×10^{11} or 6×10^{11} vg AAV9_3XFLAG-TALE$_{frat\#8}$-VP64 were injected intraperitoneally in 4-month-old YG8R mice and 6×10^{12} vg were injected in 9-day-old YG8R mice. In both groups of mice, the transgene was detected by PCR amplification with specific primers corresponding to the C terminal of the TALE gene producing a 446 pb band (Figure 2a). However, in the 4-month-old mice (group 1), the signal intensity of the PCR band was stronger in the liver and weaker in the heart and the skeletal muscle. In contrast, in the 9-day-old mice (group 2), a strong PCR amplification was observed in the three tissues (muscle, heart and liver). The 3XFLAG-TALE$_{frat\#8}$-VP64 protein (Mw ~90 kDa) was detected by western blot in the liver (4-month-old mice, group 1) and in the heart (9-day-old mice, group 2) (Figure 2b).

Increased FXN transcription induced *in vivo* by AAV9_3XFLAG-TALE$_{frat\#8}$-VP64 in the liver, heart and muscle of the YG8R mice

Northern blot analysis showed a significant increase of the FXN mRNA in the heart and muscles of the 9-day-old mice and in the liver of the 4-month-old mice (Figure 3A). Real-time reverse transcription-PCR (qRT-PCR) analyses of the same tissues expressed in terms of copy number only or as ratios with internal standards such as 18S rRNA, GAPDH, HPRT1 and ATP50 are presented in Figure 3B. These results confirmed that AAV9_3XFLAG-TALE$_{frat\#8}$-VP64 was able to stimulate *in vivo* FXN transcription. The expression ratio of the treated mice relative to the controls was similar for the four internal standards used for the analysis of this experiment.

FXN gene regulation and evaluation of the copy number by AAV9_3XFLAG-TALE$_{frat\#8}$-VP64 analyzed in five tissues of the YG8R mice (group 1)

As shown in Figure 4, no FXN mRNA upregulation was observed in the brain between the controls and the treated mice (Figure 4a). However, Figure 4b suggests an FXN mRNA upregulation in the

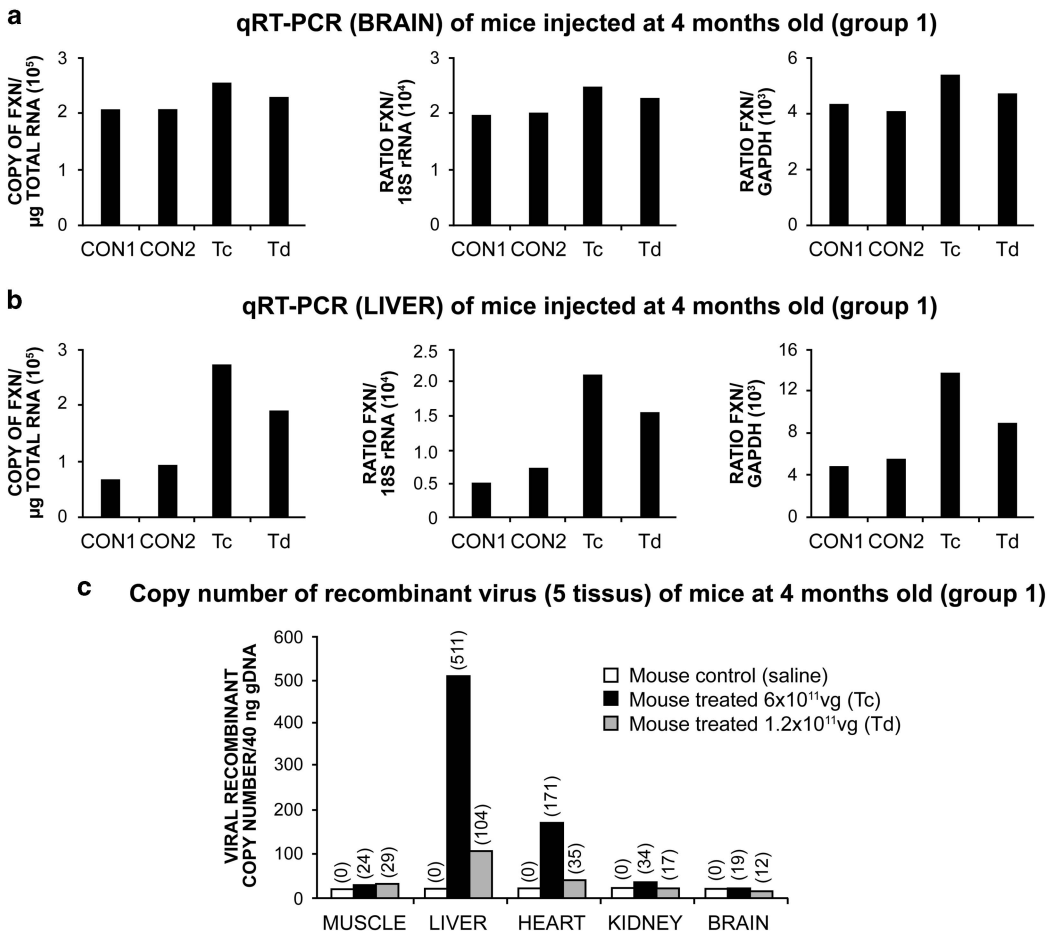

Figure 4. Effect of AAV9_3XFLAG-TALE$_{frat\#8}$-VP64 treatment on FXN mRNA analyzed by qRT-PCR in YG8R mice (group 1). (**a** and **b**) The qRT-PCR analysis of FXN mRNA from total RNA extracted from the brain and liver of two control mice (saline) and mice treated with (1.2×10^{11} vg, Td) or (6.0×10^{11} vg, Tc), respectively. The FXN mRNA is expressed as copy number per µg total RNA (left panel), ratio FXN/18 S (middle panel) and FXN/GAPDH right panel. (**c**) Illustrates the copy number (values within parentheses) of the recombinant virus found in the brain, liver, mus cle, heart, kidney of group 1 mice, followed by treatment with two different doses (1.2×10^{11} vg, Td) and (6.0×10^{11} vg, Tc). Note that each histobar represents the value of one mouse.

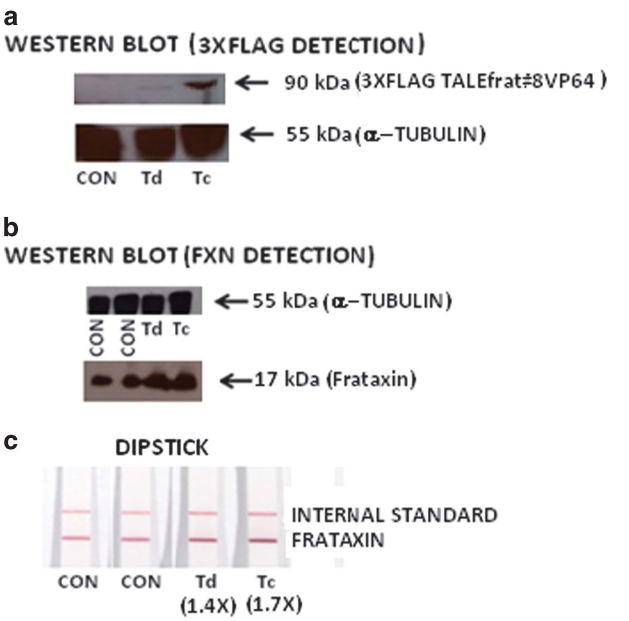

Figure 5. Detection of 3XFLAG-TALE$_{frat\#8}$-VP64 and FXN proteins in the liver of 4-month-old YG8R mice (group 1). In all figures, proteins extracted from the liver: control mice (CON) received a saline injection; mice were treated either with a diluted dose of virus (1.2×10^{11} vg, Td) or with a high dose of virus (6.0×10^{11} vg, Tc). In (**a**) the 3XFLAG-TALE$_{frat\#8}$-VP64 protein (90 kDa) was detected by western blot using an anti-3XFLAG monoclonal antibody; the expression was barely visible at the low viral dose (Td) but was more strongly expressed at the high viral dose (Tc). In (**b**), the western blot was made with a monoclonal antibody against human FXN (17 kDa). In the lower horizontal panels of (**a** and **b**), the expression of α-tubulin (55 kDa) was similar in the three samples. In (**c**), FXN expression detected with dipsticks was increased by 1.4-fold with a low dose (Td) and by 1.7-fold with a high dose (Tc) of the virus. A goat anti-mouse antibody (upper line) is included on all dipsticks as internal standard.

liver of the treated mouse at two doses tested. In the liver, there seems to be a relationship between the number of recombinant viral copy (Figure 4c) and the level of FXN mRNA upregulation (Figure 4b) in relation with the doses used: (6×10^{11} vg per mouse, Tc) and (1.2×10^{11} vg per mouse, Td). Figure 4c indicates that the liver and the heart are the main tissues targeted by the AAV9_3XFLAG-TALE$_{frat\#8}$-VP64 as indicated by the high copy number in these tissues, whereas the muscle, kidney and brain showed very low copy numbers.

Increase of the FXN protein *in vivo* by AAV9_3XFLAG-TALE$_{frat\#8}$-VP64 in the liver of 4-month-old YG8R mice (group 1)

The 3XFLAG-TALE$_{frat\#8}$-VP64 protein detected by western blot in the liver of the 4-month-old mice (Figure 5a) is parallel with the increased FXN protein expression determined either by western blot (Figure 5b) or by an enzyme-linked immunosorbent assay method (Figure 5c). These increases were ~1.4- to 1.7-fold, respectively, for diluted (1.2×10^{11} vg Td) and high (6×10^{11} vg Tc) doses. In the liver of the mice treated with a low (Td) or a high dose (Tc), a parallel increase was observed between the 3XFLAG-TALE$_{frat\#8}$-VP64 protein detected by western blot (Figure 5a), the FXN mRNA measured by qRT-PCR (Figure 4b), the FXN protein estimated by Dipstick (Figure 5c) and the recombinant virus copy number (Figure 4c) observed in the liver of the same mouse in function of the dose tested. This last observation suggests that a minimum of 100 viral copies per 40 ng gDNA (Figure 4c) is necessary in the liver to increase FXN gene expression *in vivo*.

FXN gene regulation and evaluation of the viral copy number in five tissues of the YG8R mice (group 2)

The brain of 9-day-old mice treated with a high dose (6×10^{12} vg per mouse) of recombinant virus showed no significant FXN mRNA upregulation relative to the control mice injected with saline (Figure 6a). However, the heart and muscle (Figure 6a) showed a significant upregulation of FXN mRNA following the AAV9_3XFLAG-TALE$_{frat\#8}$-VP64 treatment. No upregulation of the FXN mRNA was observed in the liver and kidney (Figure 6a) even if more than 1000 copies of the recombinant virus per 40 ng of gDNA (Figure 6b) were detected in the liver of the young mice treated with the higher viral dose. This last observation is quite different from the upregulation of FXN mRNA observed in the liver of the 4-month-old mice treated at lower doses of recombinant virus (Figures 4b and c).

Increase of FXN protein *in vivo* by AAV9 TALE$_{frat\#8}$-VP64 in the heart and the muscle of the 9-day-old YG8R mice

FXN protein increases of, respectively, 1.6- and 2.1-fold were detected by Dipstick analysis in the heart and in the skeletal muscle of 9-day-old mice (group 2) treated with 6×10^{12} vg AAV9_3XFLAGTALE$_{frat\#8}$-VP64 (Figures 7a and b). However, these increases did not reach a significant level.

DISCUSSION

The aim of the present investigation was to evaluate whether an ATF, that is, a TALE-VP64, delivered by an AAV vector was able to upregulate *in vivo* the expression of a gene as previously demonstrated *in vitro* for *FXN* gene in FRDA cells.[1] Our results demonstrated that indeed a TALE-ATF can be efficiently used *in vivo* to upregulate an important gene, such as FXN having a primordial role in FRDA, a typical haploinsufficiency disease. To date, the use of AAV vectors to transfer therapeutic gene *in vivo* is being tested in several gene therapy clinical trials.[2] The limited packaging of AAVs (~4.7 kb) is the main drawback of this delivery system for TALENs as two AAVs are needed to deliver the two TALENs required to induce a DNA double-strand break. However, in the present study, only one AAV vector was sufficient to deliver *in vivo* a TALE-TF containing only 13 RVDs and a VP64 TAD. In fact, one AAV could accommodate easily a TALE with up to 18 RVDs. The AAV serotype[23] is an option depending on the type of targeted organs for the treatment of a particular haploinsufficiency disease. AAV vector may be more advantageous to deliver *in vivo* a TALE-TF than a lentivirus vector (LV), as in the past LV failed to deliver a complete TALEN in target cells.[13] Nevertheless, the recent new versions of LVs, that is, integration-deficient lentiviral vectors[24] and non-reverse transcribable lentiviral vectors,[14] may be usable *in vivo*, but this remains to be tested.

The TALE-VP64 described in the present study has some advantages over the other potential ATFs, that is, ZFPs or dCas9 fused with a TAD. Indeed, although ZFP-TFs have been previously successfully used *in vivo* following delivery by an AAV vector,[10,25] the custom production of a high-affinity ZFP to target a specific nucleotide sequence remains difficult, requiring time-consuming and labor-intensive selection systems[26] when compared with the production of a TALE-TF.[27] The ATFs using the catalytically inactive dCas9 (4.1 kb) fused with a TAD have to be coexpressed with a gRNA.[2] The total size of these components makes it impossible to deliver them with a single AAV vector, as is the case for ZFP-ATF or TALE-TF. A recent study has demonstrated remarkably high target specificity for TALE binding to DNA and for gene upregulation by different TALE-VP64.[28]

The FRDA disease is known to produce damage and degeneration of part of the brain. In the present study, we used AAV9,

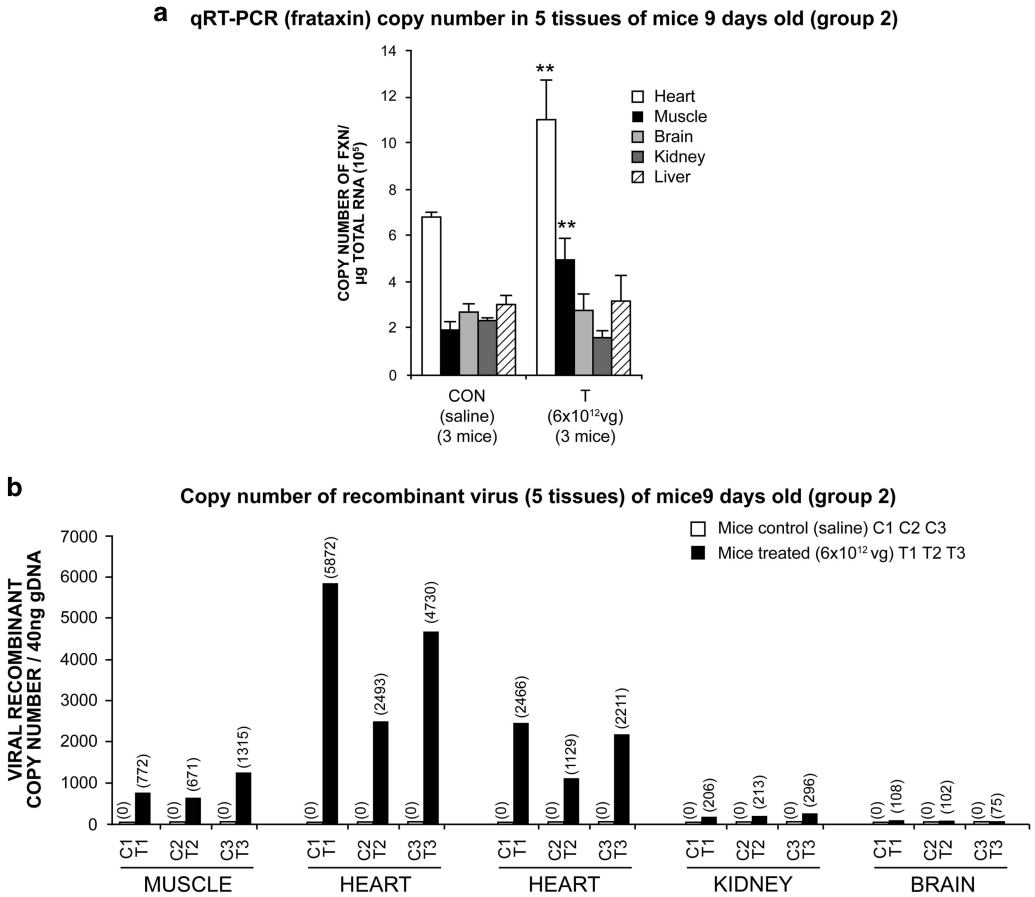

Figure 6. Effect of AAV9_3XFLAG-TALE$_{frat\#8}$-VP64 treatment on FXN mRNA analyzed in five tissues of YG8R mice (group 2) by qRT-PCR in relationship to the recombinant viral copy number found in these tissues. In (**a**), the qRT-PCR analysis of FXN mRNA from total RNA extracted from heart, muscle, brain, kidney and liver of three control mice (saline) and three mice treated with 6×10^{12} vg. The FXN mRNA is expressed in copy number per µg total RNA (ave. ± s.d.). Significant increases (**$P < 0.01$) were observed in the heart and muscle. In (**b**), the AAV copy numbers per 40 ng of gDNA in the heart and muscle following injection of 6.0×10^{12} vg per mouse are illustrated. Each histobar represents an individual mouse. The copy numbers found in the heart and muscle in (**b**) parallel the upregulation of FXN mRNA observed in (**a**) in the same tissues.

which is known to have some tropism for the brain.[29] Despite that tropism, only a low level of copy number of recombinant virus was observed in the brain of both groups of mice (Figures 4c and 6b) independently of the age and the doses of recombinant virus used. The intraperitoneal injection used in our study could explain the difficulty of AAV9_3XFLAGTALE$_{frat\#8}$-VP64 to cross the blood–brain barrier. Alternative methods of delivery, such as intravenous or intracerebroventricular, will have to be investigated in future studies. Brain optimized promoter will also have to be studied.[30] In our study, we used a ubiquitous CAG promoter to drive the expression of 3XFLAGTALE$_{frat\#8}$-VP64. This promoter may be shut down in some tissues such as the brain, and promoter optimization has been proposed.[31] Therefore, an alternative hybrid promoter, named CBX3-UCOE (0.7 kb), shown to prevent epigenetic silencing of transgene expression, could be tested in our AAV vector.[32]

A recent publication demonstrated AAV9 vector integration in newborn mouse liver leading to cancer.[33] The significance of this study for clinical use of AAV was contested as such integration has not been reported in older mice and in clinical trials.[34] However, possible viral integration in the liver by an AAV coding for a TALE-VP64 should be considered in follow-up studies. An alternative to avoid this potential liver integration problem is to use a liver-detargeted AAV9 vector.[35]

Although we have detected in the liver of both groups of treated mice abundant virus copies (Figures 4c and 6b), a functional upregulation was observed only in 4-month-old mice. The mechanism responsible for the absence of upregulation in younger mice will have to be further investigated.

In our previous study,[1] we have demonstrated an increase of the FXN mRNA and protein induced by the transfection in FRDA cells of a plasmid coding for TALE$_{frat\#8}$-VP64. In the present study, the potential therapeutic use of this ATF was further supported by an *in vivo* delivery of an AAV9 to YG8R mice, an FRDA mouse model.[36] However, as mentioned previously, many aspects should be taken into account for the development of an optimal AAV vector able to deliver safely and efficiently *in vivo* an AAV TALE-TF to its specific target, and our *in vivo* study represents only a first step towards the establishment of an *in vivo* gene therapy with a TALE-TF.

The present results showed an increase of FXN mRNA (Figures 3and b) and the FXN protein (Figures 5b and c and Figures 7a and b), proving that AAV9_3XFLAG-TALE$_{frat\#8}$-VP64 was able to significantly upregulate the expression of that gene *in vivo*. This observation is a proof-of-principle that a TALE-TF delivered by an AAV is able to upregulate *in vivo* the *FXN* gene weakly expressed owing to the presence of a long trinucleotide repeat in intron 1. In the future experiments, the VP64 TAD used in the present study may be

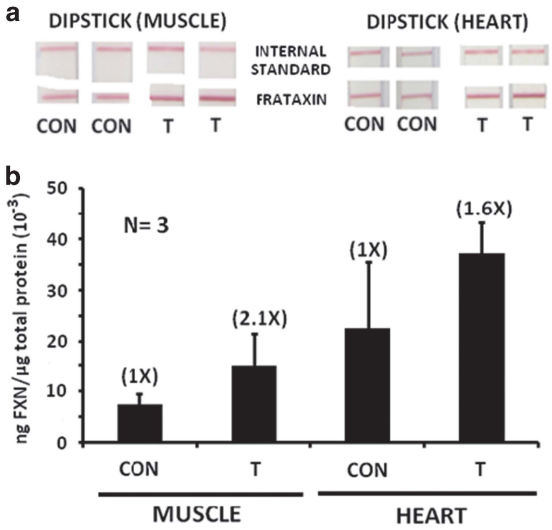

Figure 7. Dipstick analysis of the FXN protein in the heart and muscle of 9-day-old YG8R mice. (**a**) Eight Dipsticks are illustrated. On the top of each Dipstick, a positive control goat anti-mouse antibody line is included as internal standard to ensure that the same amount of proteins has been used for each assay. The four Dipsticks on the left side are dosing muscle FXN protein and four Dipsticks on the right side are dosing heart FXN protein. The illustrated Dipsticks are dosing proteins from two control (CON) mice that received a saline injection and two treated (T) 9-day-old YG8R mice (i.e., group 2) that received 1.6×10^{12} vg AAV9_3XFLAG-TALE$_{frat\#8}$-VP64. (**b**) A concentration curve was made to semiquantify the Dipstick results. The FXN protein was increased 1.6-fold in the treated (T, $N = 3$, ave. $\pm$ s.d.) heart and 2.1-fold in the treated muscles relative to control (CON, $N = 3$, ave. $\pm$ s.d.). However, these changes did not reach a significant level.

replaced by other TADs as recently described for the CRISPR/Cas9 system.[37–39]

MATERIALS AND METHODS

AAV9_3XFLAG-TALE$_{frat\#8}$-VP64 design and construction

Construction of AAV9_3XFLAG-TALE$_{frat\#8}$-VP64 was carried out starting from pCR3.1 TALE$_{frat\#8}$-VP64 plasmid.[1] This plasmid was first amplified with a TAQ DNA polymerase (NEB Inc., Ipswich, MA, USA) with the following primers: Fw, 5′-GTGAGGTCGACAGTCGCGCAGCATCA-3′ and the Rev, 5′-GGAATTCGGGCTTATTATCTAGAGTTAATCAGC-3′, containing, respectively, the restriction sites *Sal*1 and *Eco*R1. The resulting amplicon of near of 2.38 kb was cloned in a pDrive vector (Qiagen Inc., Valencia, CA, USA) (a TA cloning vector) and sequenced. The large fragment *Sal*1/*Eco*R1 was then cloned in the pAAV_TALE-TF(VP64)-BB_V3 plasmid no. 42581 (Addgene Inc., Cambridge, MA, USA; vector provided by the Zhang laboratory) digested with the same restriction enzymes. The final construct was verified by sequencing before virus production. The virus was produced at the Neurophotonics Centre (Centre de Recherche Robert Giffard, CRULRG, Quebec City, QC, Canada) and at concentrations ranging from 1.2 to 8.9×10^{13} vg ml^{-1}.

Animal use and viral TALE delivery protocol

All mice were handled in compliance with CRCHUQ guidelines approved by the Animal Care and Use committee of the Laval University. The animals of both sexes were divided into two groups: group 1 composed of four 4-month-old YG8R mice. Two control mice received intraperitoneal injection of a saline buffer. One mouse was injected intraperitoneally with 1.2×10^{11} vg AAV9_3XFLAG-TALE$_{frat\#8}$-VP64 and the other with 6.0×10^{11} vg. Group 2 was composed of six 9-day-old YG8R mice. Three control mice were injected intraperitoneally with saline buffer and the other three mice with an intraperitoneal injection of 6.0×10^{12} vg AAV9_3XFLAG-TALE$_{frat\#8}$-VP64.

PCR detection of the AAV9_3XFLAG-TALE$_{frat\#8}$-VP64 DNA and standards for estimation of copy number in different tissues

To detect the 3XFLAG-TALE$_{frat\#8}$-VP64 transgene, a portion of its C terminal was amplified with the Amplitaq Gold 360 (Thermo Fisher Scientific Inc., Waltham, MA, USA) polymerase using primers Fw, 5′-GCTGCAGCT CTTTCGTAGAGT-3′ and Rev, 5′-AGTTAATCAGCATGTCCAGGTC-3′, resulting in a 446 pb product. The PCR program was as follows: 95 °C for 10 min; 95 °C for 30 s, 58 °C for 30 s, 72 °C for 30 s for 30 cycles; final extension at 72 °C for 7 min.

A standard curve was established using known amounts of purified PCR products (10, 10^2, 10^3, 10^4, 10^5 and 10^6 copies) and a LightCycler 480 v.1.5 program provided by the manufacturer (Roche Diagnostics, Mannheim, Germany). The standard curve was used to determine the copy number of the recombinant virus in different tissues of AAV-treated mice of both groups. PCR reactions were performed in a fluorescent-based real-time PCR quantification using the LightCycler 480 (Roche Diagnostics).[40] PCR reaction results in a 143 pb product using the following primers corresponding to CAG promoter in the AAV vector: Fw, 5′-CCAAG TACGCCCCCTATTGA-3′ and Rev, 5′-GCTCACCTCGACCATGGTAAT-3′. The PCR reactions were carried out with 40 ng of genomic DNA using the following parameters: 45 cycles, denaturation at 95 °C for 10 s, annealing at 59 °C for 10 s, elongation at 72 °C for 14 s and then 74 °C for 5 s (reading).

Northern blot and qRT-PCR analysis in the liver, heart and skeletal muscle

Total RNA was isolated from tissues quickly frozen in liquid nitrogen at − 80 °C until use. RNA was extracted with Trizol (Life Technology Inc., Waltham, MA, USA) as recommended by the manufacturer. Frozen tissues were homogenized in the Qiazol buffer (Qiagen, Germantown, MD, USA). The total RNA was extracted one time with phenol and the aqueous phase was passed through the RNeasy Micro Kit On-column DNase (Qiagen, Hilden, Germany) treatment following the manufacturer's instructions. The total RNA was measured using a NanoDrop ND-1000 Spectrophotometer (NanoDrop Technologies, Wilmington, DE, USA) and the RNA quality was assayed on an Agilent BioAnalyzer 2100 (Agilent Technologies, Santa Clara, CA, USA). For Northern blot analysis, 10 or 15 µg of RNA was loaded per lane on a 1.2% agarose gel containing 3.5% formaldehyde in 1× MOPS buffer (MOPS 0.02 M, sodium acetate 5 mM, EDTA 1 mM, pH 7.0) containing Red Safe Nucleic Acid *Staining* Solution (0.1 µl ml^{-1} of gel). The Northern gel was electrophoresed at 90 V in 1× MOPS buffer containing Red Safe at 0.066 µl ml^{-1}. Alkaline RNA transfer (transfer on Biodyne B membrane and washings) was carried out during 2–3 h as reported previously.[41] FXN cDNA (408 pb) covering exons 2–5 and 18 S cDNA (402 pb) were produced by PCR amplification of DNA extracted from a human fibroblast culture and used as probes for the hybridization step. The hybridization was performed as follows: human FXN and 18 S rRNA cDNAs at 100 ng each were radiolabeled with ^{32}P (dCTP, 3000 Ci mmol^{-1}) using NEBlot Kit–Random Priming Reaction (New England Biolab, Ipswich, MA, USA). These radioactive probes were purified on GFX MicroSpin column (GE Healthcare, Mississauga, ON, Canada); the prehybridization and hybridization solutions were the same (1× SSPE, 2× Denhardt's, 10% dextran sulfate, 1% sodium dodecyl sulfate (SDS), salmon DNA 100 µg ml^{-1}). Following 3 h of prehybridization at 65 °C, the probes were denatured by heating for 5 min at 95 °C and then chilled on ice for 5 min, and then placed directly in the roller bottle in the oven at 65 °C for overnight hybridization. This was followed by three 10 min washing steps at 65 °C: once in 2×SSC/0.1% SDS and two times in 0.2×SSC/0.1% SDS. The washed membranes were then lightly dried and exposed on an X-ray film for different times in the freezer at − 80 °C.

qRT-PCR for the FXN mRNA and for four internal standards (i.e., GAPDH, HPRT1, 18 S rRNA and ATP50) was carried out using a technique previously described by Luu-The *et al.*[40] and Chapdelaine *et al.*[1] Briefly, the total RNA to analyze was extracted from tissues as described above and 20 ng was used for qRT-PCR analysis.

Protein extraction and analysis of FXN and of 3XFLAG-TALE$_{frat\#8}$-VP64 by western blot

Tissue protein extraction and western blot analysis for FXN and the 3XFLAG were carried out as described by Chapdelaine *et al.*,[1] except that the protein extraction was carried out from tissues frozen in nitrogen liquid kept at − 80 °C and grinded with a pestle in a mortar.

A small amount of the resulting powder was lysed in a buffer as described above for protein extraction. The following first antibodies were used for western blot analysis: for FXN, anti-FXN antibody (18A5DB1) (ab110328; Abcam Inc., Cambridge, MA, USA) used at 3–5 μg ml^{-1}; for 3XFLAG, monoclonal mouse anti-Flag M2 antibody (F1804; Sigma-Aldrich Inc., St Louis, MO, USA) used at 1/2000; for α-tubulin, monoclonal α-tubulin clone B-5-1-2 (T5168, Sigma-Aldrich Inc.) used at 1/4000. The second antibody was a goat anti-mouse coupled with peroxidase (Jackson Laboratory, Bar Harbor, ME, USA) used at 1/10 000 as described previously.[1]

Quantification of the FXN protein in the mouse tissue by enzyme-linked immunosorbent assay (Dipstick)

The human FXN protein of the liver, heart and skeletal muscle was quantified using the Dipstick Array (Abcam; cat. no. ab109881). This is an immunologic sandwich assay using two monoclonal antibodies specific for two antigens present in the mature form of FXN, which have been described previously.[42] One antibody is immobilized on the nitrocellulose membrane in a thin line perpendicular to the length of the dipstick while the other is gold-conjugated, which gives the red signal proportional to the FXN concentration. A concentration curve using 75 – 600 pg human FXN protein (Abcam Inc.; cat. no. ab110353) was carried out to 'semiquantify' the density of the FXN band. The signal intensity was measured and analyzed using the Spot-Denso software on Alpha Imager 2000 system (Cell Biosciences, Inc., Santa Clara, CA, USA).

CONFLICT OF INTEREST

JPT is conducting research on gene therapy for Friedreich's ataxia under a research contract with Amorchem Inc. and a patent for such treatment has been applied for by his university. The other authors declare no conflict of interest.

REFERENCES

1 Chapdelaine P, Coulombe Z, Chikh A, Gerard C, Tremblay JP. A potential new therapeutic approach for Friedreich ataxia: induction of frataxin expression with TALE proteins. *Mol Ther Nucleic acids* 2013; **2**: e119.
2 Thakore PI, Gersbach CA. Genome engineering for therapeutic applications. In: Laurence J, Frankling M (ed). *Translating Gene Therapy to the Clinic Techniques and Approaches*. Academic Press: London, UK, 2015, pp 27–39.
3 Boch J, Bonas U. *Xanthomonas* AvrBs3 family-type III effectors: discovery and function. *Annu Rev Phytopathol* 2010; **48**: 419–436.
4 Bogdanove AJ, Schornack S, Lahaye T. TAL effectors: finding plant genes for disease and defense. *Current opinion in plant biology* 2010; **13**: 394–401.
5 Mak AN, Bradley P, Cernadas RA, Bogdanove AJ, Stoddard BL. The crystal structure of TAL effector PthXo1 bound to its DNA target. *Science* 2012; **335**: 716–719.
6 Deng D, Yan C, Pan X, Mahfouz M, Wang J, Zhu JK *et al.* Structural basis for sequence-specific recognition of DNA by TAL effectors. *Science* 2012; **335**: 720–723.
7 Zhang F, Cong L, Lodato S, Kosuri S, Church GM, Arlotta P. Efficient construction of sequence-specific TAL effectors for modulating mammalian transcription. *Nat Biotechnol* 2011; **29**: 149–154.
8 Gaj T, Gersbach CA, Barbas CF III. ZFN, TALEN, and CRISPR/Cas-based methods for genome engineering. *Trends Biotechnol* 2013; **31**: 397–405.
9 Lombardo A, Genovese P, Beausejour CM, Colleoni S, Lee Y-L, Kim KA *et al.* Gene editing in human stem cells using zinc finger nucleases and integrase-defective lentiviral vector delivery. *Nat Biotechnol* 2007; **25**: 1298–1306.
10 Li H, Haurigot V, Doyon Y, Li T, Wong SY, Bhagwat AS *et al. In vivo* genome editing restores haemostasis in a mouse model of haemophilia. *Nature* 2011; **475**: 217–221.
11 Bedell VM, Wang Y, Campbell JM, Poshusta TL, Starker CG, Krug RG II *et al. In vivo* genome editing using a high-efficiency TALEN system. *Nature* 2012; **491**: 114–118.
12 Jankele R, Svoboda P. TAL effectors: tools for DNA targeting. *Brief Funct Genomics* 2014; **13**: 409–419.
13 Holkers M, de Vries AA, Goncalves MA. Nonspaced inverted DNA repeats are preferential targets for homology-directed gene repair in mammalian cells. *Nucleic Acids Res* 2012; **40**: 1984–1999.
14 Mock U, Riecken K, Berdien B, Qasim W, Chan E, Cathomen T *et al.* Novel lentiviral vectors with mutated reverse transcriptase for mRNA delivery of TALE nucleases. *Scientific Rep* 2014; **4**: 6409.
15 Wu Z, Asokan A, Samulski RJ. Adeno-associated virus serotypes: vector toolkit for human gene therapy. *Mol Ther* 2006; **14**: 316–327.
16 Bish LT, Morine K, Sleeper MM, Sanmiguel J, Wu D, Gao G *et al.* Adeno-associated virus (AAV) serotype 9 provides global cardiac gene transfer superior to AAV1, AAV6, AAV7, and AAV8 in the mouse and rat. *Hum Gene Ther* 2008; **19**: 1359–1368.
17 Fu H, Dirosario J, Killedar S, Zaraspe K, McCarty DM. Correction of neurological disease of mucopolysaccharidosis IIIB in adult mice by rAAV9 trans-blood–brain barrier gene delivery. *Mol Ther* 2011; **19**: 1025–1033.
18 Dayton RD, Wang DB, Klein RL. The advent of AAV9 expands applications for brain and spinal cord gene delivery. *Expert Opin Biol Ther* 2012; **12**: 757–766.
19 Aschauer DF, Kreuz S, Rumpel S. Analysis of transduction efficiency, tropism and axonal transport of AAV serotypes 1, 2, 5, 6, 8 and 9 in the mouse brain. *PLoS One* 2013; **8**: e76310.
20 Pandolfo M. Friedreich ataxia. In: Subramony SH, Dürr A (eds). *Handbook of Clinical Neurology*, 3rd edn, vol. 103. Elsevier: Amsterdam, 2012, pp 275–294.
21 Campuzano V, Montermini L, Lutz Y, Cova L, Hindelang C, Jiralerspong S *et al.* Frataxin is reduced in Friedreich ataxia patients and is associated with mitochondrial membranes. *Hum Mol Genet* 1997; **6**: 1771–1780.
22 Koeppen AH. Friedreich's ataxia: pathology, pathogenesis, and molecular genetics. *J Neurol Sci* 2011; **303**: 1–12.
23 Zincarelli C, Soltys S, Rengo G, Rabinowitz JE. Analysis of AAV serotypes 1-9 mediated gene expression and tropism in mice after systemic injection. *Mol Ther* 2008; **16**: 1073–1080.
24 Suwanmanee T, Hu G, Gui T, Bartholomae CC, Kutschera I, von Kalle C *et al.* Integration-deficient lentiviral vectors expressing codon-optimized R338L human FIX restore normal hemostasis in Hemophilia B mice. *Mol Ther* 2014; **22**: 567–574.
25 Laganiere J, Kells AP, Lai JT, Guschin D, Paschon DE, Meng X *et al.* An engineered zinc finger protein activator of the endogenous glial cell line-derived neurotrophic factor gene provides functional neuroprotection in a rat model of Parkinson's disease. *J Neurosci* 2010; **30**: 16469–16474.
26 Mercer AC, Gaj T, Fuller RP, Barbas CF III. Chimeric TALE recombinases with programmable DNA sequence specificity. *Nucleic Acids Res* 2012; **40**: 11163–11172.
27 Zhang Z, Li D, Xu H, Xin Y, Zhang T, Ma L *et al.* A simple and efficient method for assembling TALE protein based on plasmid library. *PLoS One* 2013; **8**: e66459.
28 Polstein LR, Perez-Pinera P, Kocak DD, Vockley CM, Bledsoe P, Song L *et al.* Genome-wide specificity of DNA binding, gene regulation, and chromatin remodeling by TALE- and CRISPR/Cas9-based transcriptional activators. *Genome Res* 2015; **25**: 1158–1169.
29 Manfredsson FP, Rising AC, Mandel RJ. AAV9: a potential blood–brain barrier buster. *Mol Ther* 2009; **17**: 403–405.
30 McLean JR, Smith GA, Rocha EM, Hayes MA, Beagan JA, Hallett PJ *et al.* Widespread neuron-specific transgene expression in brain and spinal cord following synapsin promoter-driven AAV9 neonatal intracerebroventricular injection. *Neurosci Lett* 2014; **576**: 73–78.
31 Gray SJ, Foti SB, Schwartz JW, Bachaboina L, Taylor-Blake B, Coleman J *et al.* Optimizing promoters for recombinant adeno-associated virus-mediated gene expression in the peripheral and central nervous system using self-complementary vectors. *Hum Gene Ther* 2011; **22**: 1143–1153.
32 Muller-Kuller U, Ackermann M, Kolodziej S, Brendel C, Fritsch J, Lachmann N *et al.* A minimal ubiquitous chromatin opening element (UCOE) effectively prevents silencing of juxtaposed heterologous promoters by epigenetic remodeling in multipotent and pluripotent stem cells. *Nucleic Acids Res* 2015; **43**: 1577–1592.
33 Chandler RJ, LaFave MC, Varshney GK, Trivedi NS, Carrillo-Carrasco N, Senac JS *et al.* Vector design influences hepatic genotoxicity after adeno-associated virus gene therapy. *J Clin Invest* 2015; **125**: 870–880.
34 Berns KI, Byrne BJ, Flotte TR, Gao G, Hauswirth WW, Herzog RW *et al.* Adeno-associated virus type 2 and hepatocellular carcinoma? *Hum Gene Ther* 2015; **26**: 779–781.
35 Pulicherla N, Shen S, Yadav S, Debbink K, Govindasamy L, Agbandje-McKenna M *et al.* Engineering liver-detargeted AAV9 vectors for cardiac and musculoskeletal gene transfer. *Mol Ther* 2011; **19**: 1070–1078.
36 Perdomini M, Hick A, Puccio H, Pook MA. Animal and cellular models of Friedreich ataxia. *J Neurochem* 2013; **126**(Suppl 1): 65–79.
37 Tanenbaum ME, Gilbert LA, Qi LS, Weissman JS, Vale RD. A protein-tagging system for signal amplification in gene expression and fluorescence imaging. *Cell* 2014; **159**: 635–646.
38 Hilton IB, D'Ippolito AM, Vockley CM, Thakore PI, Crawford GE, Reddy TE *et al.* Epigenome editing by a CRISPR-Cas9-based acetyltransferase activates genes from promoters and enhancers. *Nat Biotechnol* 2015; **33**: 510–517.

39 Chavez A, Scheiman J, Vora S, Pruitt BW, Tuttle M, PRI E *et al*. Highly efficient Cas9-mediated transcriptional programming. *Nat Methods* 2015; **12**: 326–328.

40 Luu-The V, Paquet N, Calvo E, Cumps J. Improved real-time RT-PCR method for high-throughput measurements using second derivative calculation and double correction. *Biotechniques* 2005; **38**: 287–293.

41 Green MR, Sambrook J. Northern blotting: Transfer of denatured RNA to membranes. In: Sambrook J, Russell DW (eds). *Molecular Cloning: A Laboratory Manual*. Cold Spring Harbor Laboratory Press: Cold Spring Harbor, NY, USA, 2001, pp 7.35–7.41.

42 Gérard C, Xiao X, Filali M, Coulombe Z, Arsenault M, Couet J *et al*. An AAV9 coding for frataxin clearly improved the symptoms and prolonged the life of Friedreich ataxia mouse models. *Mol Ther Methods Clin Dev* 2014; **1**: 1–11.